INTERNATIONAL JOURNAL OF CLIMATOLOGY
Int. J. Climatol. (2010)
Published online in Wiley Online Library
(wileyonlinelibrary.com) DOI: 10.1002/joc.2258

RMetS
Royal Meteorological Society

Variations and prediction of the annual number of tropical cyclones affecting Korea and Japan

Andy Zung-Ching Goh and Johnny C. L. Chan*
Guy Carpenter Asia-Pacific Climate Impact Centre, School of Energy and Environment, City University of Hong Kong, Hong Kong, China

ABSTRACT: This paper investigates the factors affecting the annual number of tropical cyclones (TCs) passing within 100 km of the coast of Korea and Japan (KJ). Using a training set consisting of the coefficients of empirical orthogonal functions of these factors between 1965 and 2005, equations are derived to predict the annual number of these TCs over the whole season in April, and to update this prediction for the July-November (JN) season in June. Results show that the El Niño-Southern Oscillation (ENSO) plays a key role in determining the behaviour of TCs affecting KJ, with more TCs affecting the region during El Niño and less during La Niña. This difference can be attributed to ENSO modifying the flow patterns, which in turn affects TC behaviour. The prediction equations suggest that the 500-hPa geopotential height is more important in determining the number of TCs affecting KJ in the whole season, while both the 850-hPa geopotential height and 850-hPa vorticity play a role in the JN season. Both prediction schemes are able to produce acceptable results, with forecast skills of 42.3 and 33.3% over climatology for the whole, and JN seasons, respectively. The predicted TC number for 2006, 2007, and 2008 are also mostly accurate to within one standard deviation of the observed number. Copyright © 2010 Royal Meteorological Society

KEY WORDS tropical cyclone; tropical cyclone landfall; seasonal forecasting

Received 12 November 2009; Revised 12 October 2010; Accepted 19 October 2010

1. Introduction

Tropical cyclones (TCs) are one of the most destructive natural phenomena around the world. The aftermath of a TC making landfall can be devastating, especially to the people living along its path and along the coast. It is therefore imperative to understand the behaviour of landfalling TCs.

Various studies have been carried out covering different aspects of landfalling TCs, including rainfall distribution (e.g. Kimball, 2008), maximum wind speed and decay (e.g. Kaplan and DeMaria, 1995), and convective properties (e.g. Chan *et al*., 2004). Some research has also been conducted on predicting the number of TCs making landfall, especially in the Atlantic basin (e.g. Lehmiller *et al*., 1997; Bove *et al*., 1998), with a few investigating the topic for the western North Pacific (WNP) (e.g. Wu *et al*., 2004), and even fewer dedicated solely to specific basins, such as the South China Sea (SCS) (e.g. Liu and Chan, 2003, Goh and Chan, 2010a) or the East China Sea (e.g. Kim *et al*., 2009), or a specific country (e.g. Choi *et al*., 2009 for Korea). This study will be the first to develop a real-time forecasting scheme for the Korea and Japan region.

Gray (1968, 1979) suggested several dynamic and thermodynamic factors crucial to the formation of TCs, which formed the basis for Goh and Chan's (2010b) investigation of the interannual and interdecadal variations of TCs in the SCS. The authors identified seven factors related to TC behaviour in the SCS, and the effects of these factors are in fact extended from the WNP. The seven factors can be divided into two groups: steering factors (500-hPa geopotential height and zonal wind) and genesis factors (850-hPa geopotential height and relative vorticity, 200-hPa divergence, 200–850 hPa vertical wind shear, and 1000–500-hPa moist static energy).

In addition, the El Niño-Southern Oscillation (ENSO) phenomenon has long been known to have an impact on TC behaviour in the WNP (e.g. Chan, 1985, 2000, 2005; Li, 1988; Wang and Chan, 2002). Nakazawa and Rajendran (2007) identified ENSO as one of the dominant modes affecting TC tracks in the WNP. Goh and Chan's (2010b) study also suggested that TCs tend to recurve towards Japan during El Niño (EN) and move westwards towards the SCS during La Niña (LN). These results suggest that ENSO could also be a factor in determining the number of TCs affecting Korea and Japan (KJ). Therefore, the seven factors, along with the ENSO index, will form the basis of investigation for this study.

Data used in this study are listed in Section 2. Section 3 is an analysis of the TC data, and factors affecting the behaviour of the TCs are studied in Section 4. Section 5 introduces the method of developing and assessing the prediction schemes, and Section 6 shows the prediction schemes at work. Finally, some discussion and concluding remarks are given in Section 7.

* Correspondence to: Johnny C. L. Chan, Guy Carpenter Asia-Pacific Climate Impact Centre, School of Energy and Environment, City University of Hong Kong, Tat Chee Avenue, Kowloon, Hong Kong, China. E-mail: johnny.chan@cityu.edu.hk

2. Data and approach

2.1. Data

Six-hourly TC position data and atmospheric data in this study are from the Hong Kong Observatory and the National Centers for Environmental Prediction–National Center for Atmospheric Research (NCEP-NCAR) Reanalysis Project (Kalnay *et al*., 1996), respectively. ENSO data are available from the Climate Prediction Center of the US National Weather Service (http://www.cpc.ncep.noaa.gov/products/analysis_monitoring/ensostuff/ensoyears.shtml). As previous research has suggested the existence of uncertainties in data before 1965 (e.g. Song *et al*., 2002; Wu *et al*., 2005), this study covers the period between 1965 and 2005.

2.2. Data categorization

The area of interest in this study covers the mainland of Korea and Japan, as well as the oceans within about 100 km of these two countries, as highlighted in Figure 1. TCs that pass within about 100 km from the mainland of Korea and Japan are also included because the most damaging winds from a TC are found at a distance from its centre, that is, the radius of maximum wind, and this radius is found to be about 100 km in most tropical cyclones (Shea and Gray, 1973). When a straight line joining two consecutive 6-hourly positions of a TC crosses the above defined boundary, that TC would be regarded as having affected these two land masses. TCs that first crossed this boundary, then moved out, and subsequently entered the region again would only be counted once.

To decide whether a certain year is an EN or a LN year, the ENSO index as defined by Trenbeth (1997) is used. The index is sea surface temperature based, and is calculated over the Niño-3.4 region (5 °S–5°N, 120 °W–170 °W). If the index is above +0.4, that year would be considered an EN year, whereas it would be a LN year if the index is below −0.4. For this dataset, there are 12 EN and 13 LN years.

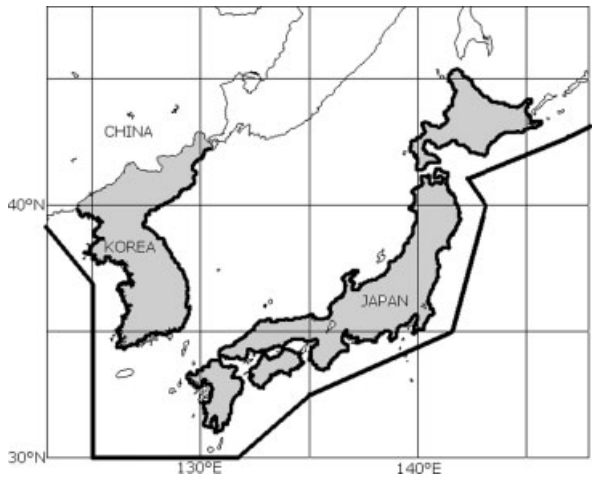

Figure 1. Area enclosed by thick black straight lines indicates the area of investigation in this study. TCs entering this area are considered to have made landfall over Korea and Japan.

3. Behaviour of TCs affecting KJ

The TC season for KJ is from May to November, with the total number in July, August, and September (N_P) accounting for 85% of all TCs in this study (Figure 2). These three months will be defined as the 'peak season' in this study. On average, the total number of TCs affecting KJ for the whole season (N_W) during the period of 1965–2005 is 4.24, while that of the peak season is 3.56.

As mentioned above, ENSO has also been pointed out to be a factor affecting N_W, and this is in fact the case. The average N_W during EN and LN is 5.08 and 3.38, respectively, a difference statistically significant at 95% confidence level, while the average N_P during these two phases of the ENSO is 4.08 and 2.92, respectively, significant at the 90% confidence level.

Both the N_W and N_P time series (Figure 3(a) and (b), respectively) show an increasing trend of 2.44 and 0.54 TCs per 100 years, respectively, based on Santer *et al*.'s (2000) method, but neither time series shows a statistically significant long-term trend. This result concurs with recent findings that, although the TC activity along the east coast of China and near Japan was higher between 1998 and 2005 (Liu and Chan, 2008), the number of TCs making landfall in the Korean Peninsula and Japan show no significant linear trend (Chan and Xu, 2009).

4. Factors affecting TCs affecting KJ

To determine the factors responsible for the behaviour of TCs affecting KJ, correlation maps are obtained for the whole season between N_W and the seven factors mentioned in Section 1, namely 500-hPa-zonal wind (500U), 200-hPa divergence (DIV), 500-hPa geopotential height (500H), 850-hPa geopotential height (850H), moist static energy (MSE), 200–850-hPa shear (SHEAR), and 850-hPa vorticity (VOR) (Figure 4). It can be seen that N_W has statistically significant correlation with most of these factors over the WNP. Specifically, the correlation between N_W and 500H (Figure 4(a)) and 500U (Figure 4(b)) seems to suggest that the steering flow could be an important factor in determining the number of TCs making affecting KJ.

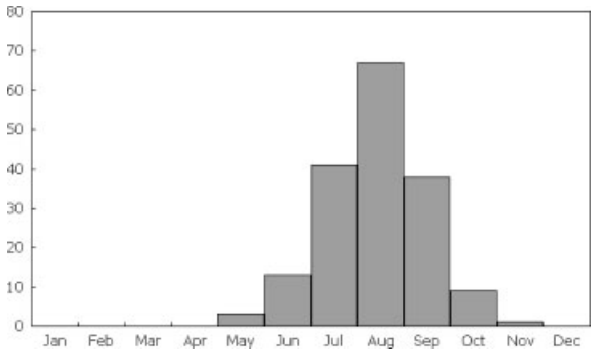

Figure 2. Monthly distribution of TCs making landfall over Korea and Japan.

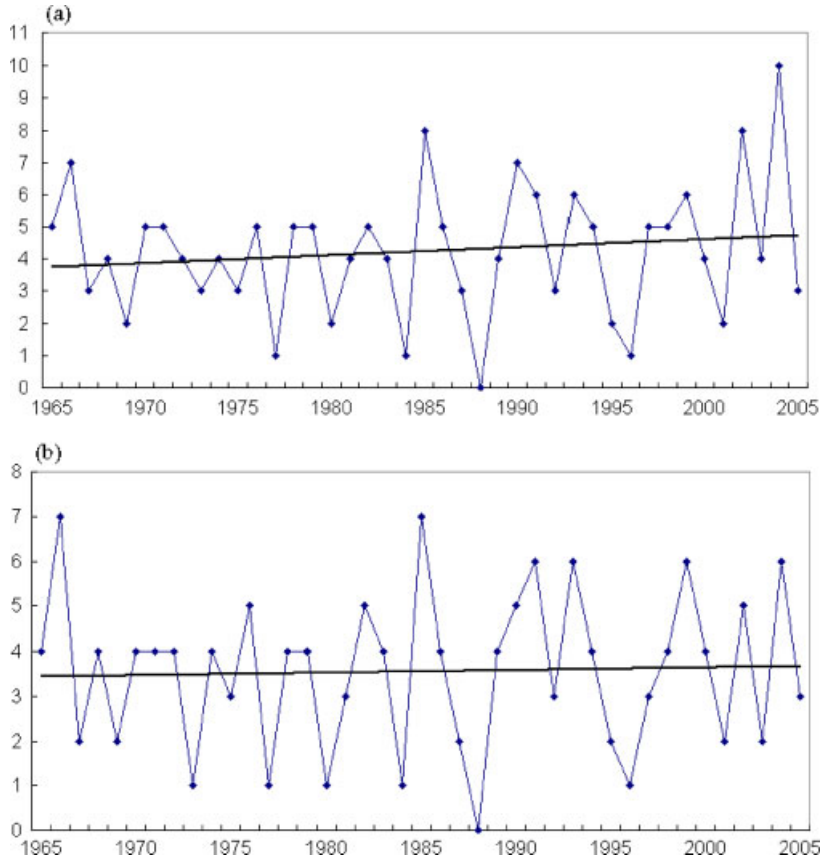

Figure 3. Number of TCs making landfall over Korea and Japan during (a) the whole season (N_W), and (b) the peak season (N_P). The solid straight line indicates the trend. This figure is available in colour online at wileyonlinelibrary.com/journal/joc

As suggested previously, ENSO was found to be one of the factors contributing to the behaviour of TCs affecting KJ. To illustrate this case, a composite analysis was performed to investigate the differences in the flow patterns of the seven factors during EN and LN and to determine the reason for the difference in the number of TCs affecting KJ during these two phases. This exercise would only be done for the peak season, as the majority of TCs affect KJ during these three months, and the flow patterns over this period should be able to provide a good insight.

4.1. EN

Figure 5 shows the flow patterns of the seven factors during EN. Recall that there are more TCs affecting KJ during this phase of the ENSO. Focusing first on the genesis factors. It can be seen that 850H shows negative anomaly over the entire WNP (Figure 5(c)), an indication of a more favourable environment for TC formation over the basin. At the same time, the anomaly of MSE (Figure 5(e)) is positive over the TC genesis region in the WNP. In addition, south of the 20°N latitude, positive anomalies of DIV (Figure 5(d)) and VOR (Figure 5(g)), and negative anomaly of SHEAR (Figure 5(f)) can be found. These all indicate favourable conditions for TC genesis. Thus, all the genesis factors suggest that TC formation is enhanced in the WNP during EN, which helps explain the reason for more TCs affecting KJ.

The reason for the above-normal N_P is even clearer with a study of the steering factors. The pattern of 500H (Figure 5(a)) shows a strong anomalous low centred over Korea, thus anomalous southerlies would be found over the WNP. These southerlies would steer TCs northwards towards the area south of Japan. At the same time, the flow pattern of 500U (Figure 5(b)) shows anomalous easterlies south of around 25°N, and anomalous westerlies north of that latitude. The joint effect of these two factors would cause TCs to follow a re-curving track and travel into the KJ region, thus contributing to a larger N_P. Thus, combining the effects of the genesis and steering factors, the reasons for more TCs affecting KJ include more TCs forming in the WNP, and flow patterns causing TCs to re-curve and travel towards KJ.

4.2. LN

Fewer TCs tend to affect KJ during LN. It can be seen from the flow patterns of the seven factors in Figure 6 that the situation during LN is generally opposite to that of EN, as all genesis factors seem to suggest unfavourable conditions for TC formation over the WNP. For example, the pattern of 850H shows positive anomaly over much of the WNP (Figure 6(a)), while negative anomaly of MSE (Figure 6(e)) can be seen south of 25°N. Moreover, positive anomaly of SHEAR is found south of 20°N (Figure 6(f)), while negative anomaly of DIV (Figure 6(d)) and VOR (Figure 6(g)) can be seen

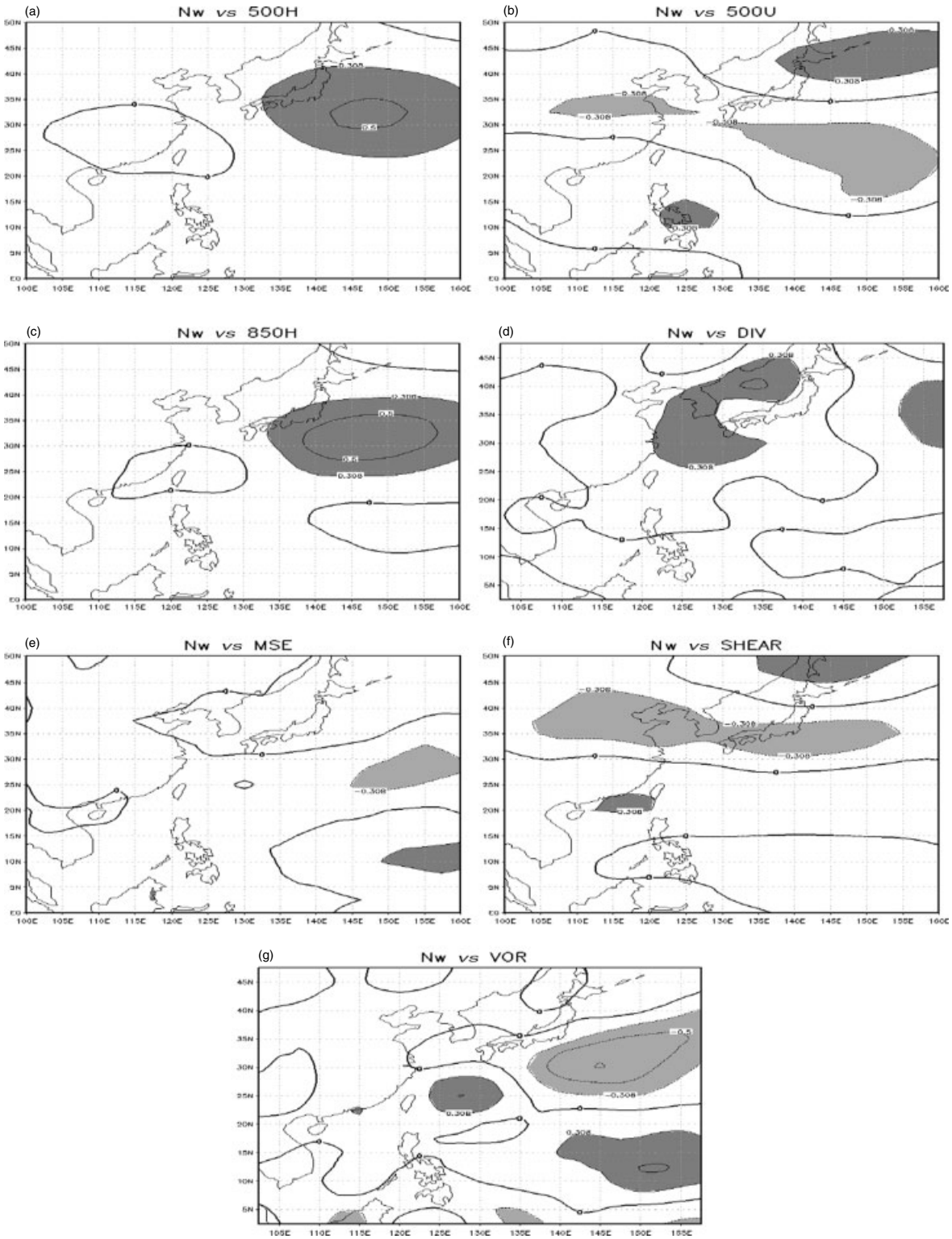

Figure 4. Correlation between N_W and the various factors affecting TC behaviour in the whole season. Solid and dotted lines indicate positive and negative values respectively, while dark and light shaded areas indicate positive and negative correlations of 95% statistical significance respectively. (a) 500H, (b) 500U, (c) 850H, (d) DIV, (e) MSE, (f) SHEAR, and (g) VOR.

in the same area, which all point to a less favourable environment for TC genesis, and hence, fewer TCs are formed over the WNP during LN.

In addition, easterly anomalies are seen in the 500U pattern south of around 15°N (Figure 6(b)), which helps to steer TCs westwards instead of towards KJ. At the same time, the pattern of 500-H reveals a positive height anomaly centred north of Korea (Figure 6(a)). This would induce an anomalous anticyclonic flow over the WNP, which again steers TCs westwards rather than allowing them to re-curve towards KJ. A smaller number of TCs formed in the WNP along with a steering flow causing

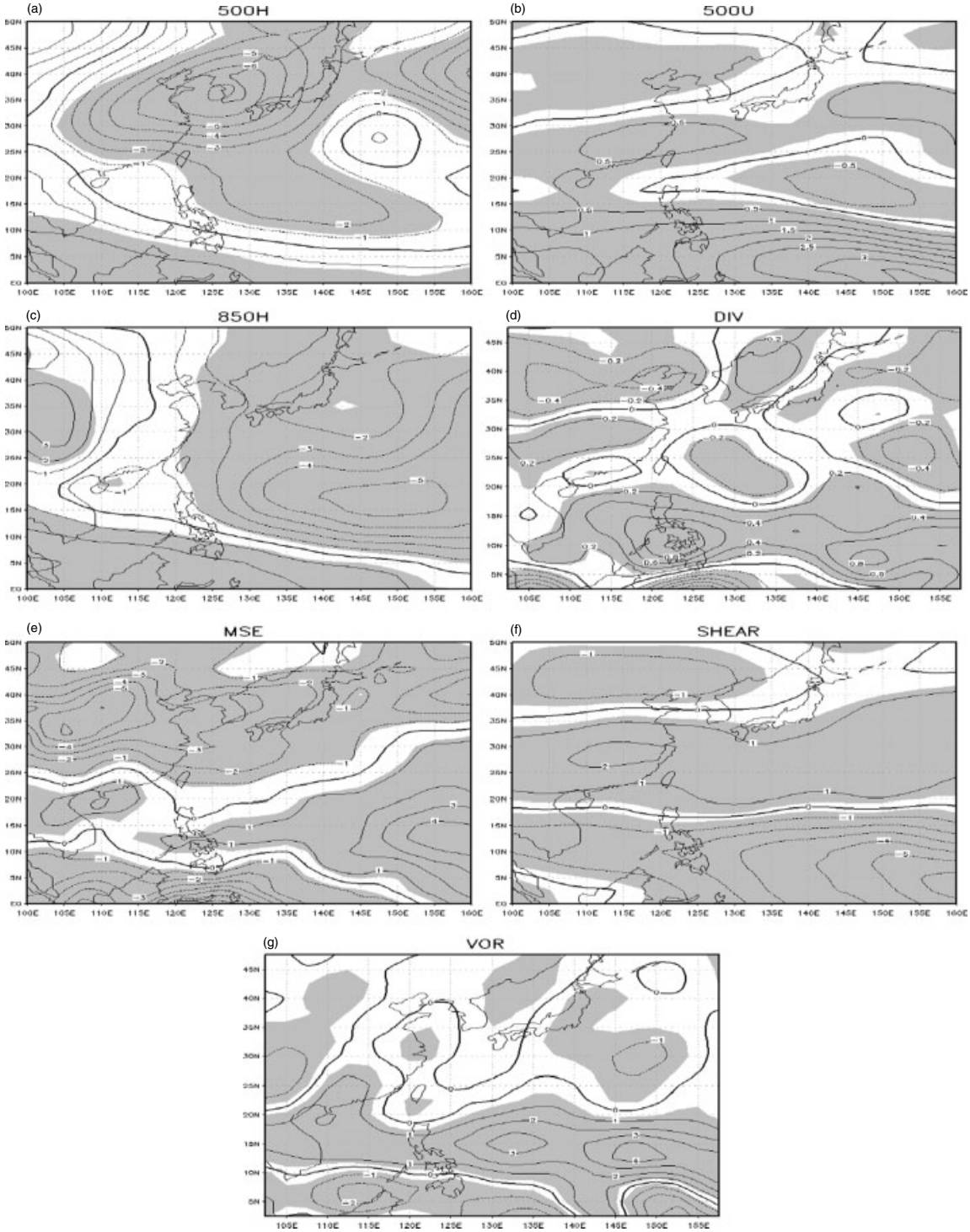

Figure 5. Anomaly patterns of the seven factors in the peak season during EN. Solid and dotted lines indicate positive and negative values, respectively. (a) 500H (Unit: gpm), (b) 500U (Unit: m s^{-1}), (c) 850H (Unit: gpm), (d) DIV (Unit: $\times 10^{-6}$ s^{-1}), (e) MSE (Unit: $\times 10^{6}$ W m^{2}), (f) SHEAR (Unit: m s^{-1}), and (g) VOR (Unit: $\times 10^{-6}$ s^{-1}). Shaded areas indicate values are statistically significant at the 95% confidence level.

TCs to travel westwards can both account for the lower N_W observed during LN.

5. Predicting the number of TCs affecting KJ

5.1. Constructing the scheme

Two prediction schemes are developed for predicting the number of TCs affecting KJ. An initial forecast for the number over the whole season (N_W) will be made in April, with an updated number (N_J) for the July–November (JN) season to be made in June.

The first three empirical orthogonal functions (EOFs) of monthly anomalies of the seven factors mentioned in Section 1, namely 500-hPa zonal wind (500U), 200-hPa divergence (DIV), 500-hPa geopotential height (500H), 850-hPa geopotential height (850H), moist static energy

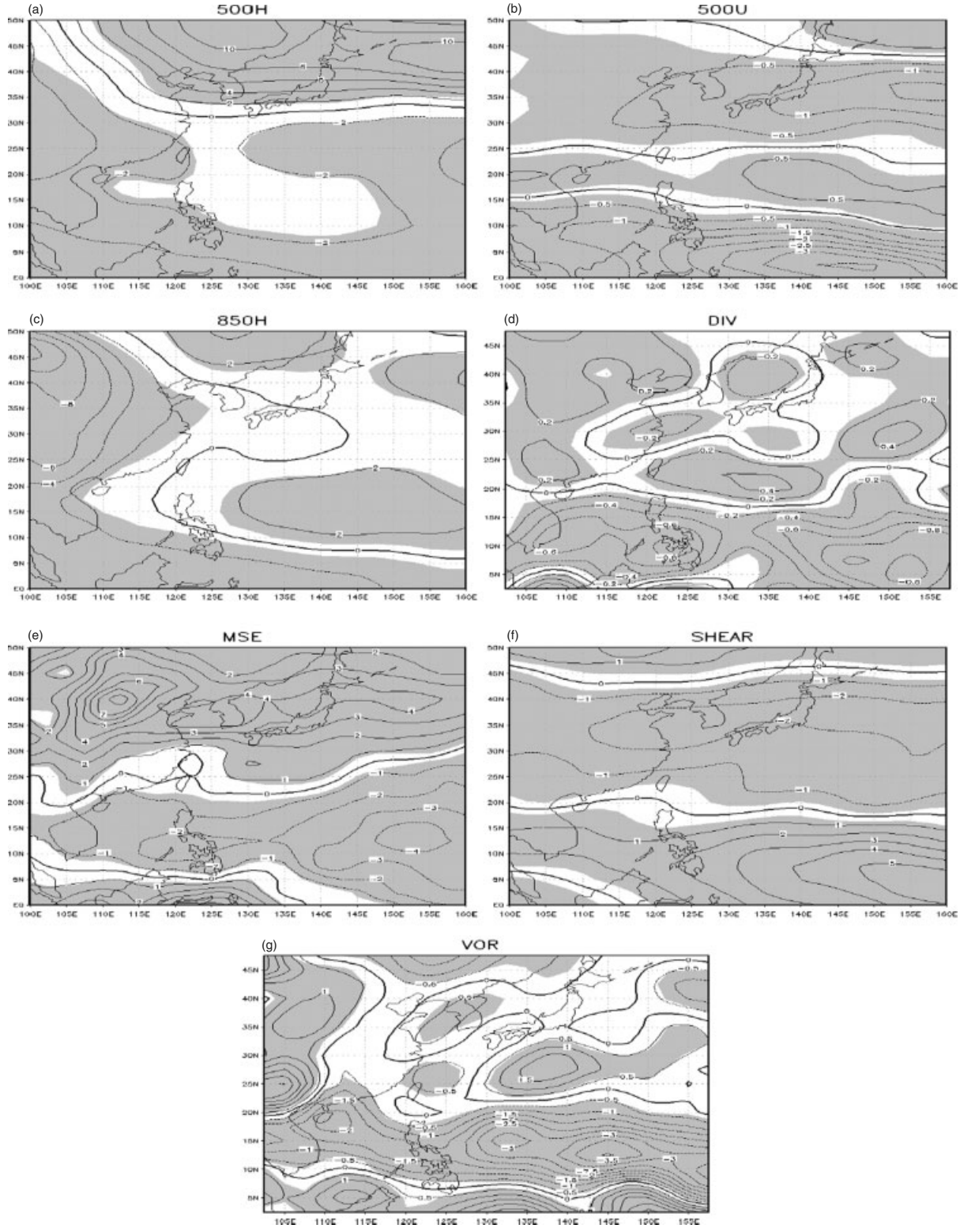

Figure 6. Same as Figure 5, except for LN.

(MSE), 200–850-hPa shear (SHEAR), and 850-hPa vorticity (VOR), plus the ENSO index, are used as predictors. The temporal range for the seven factors is from September of the previous year to March (for April prediction) or May (for June prediction) of the current year, while that for the ENSO index is extended to January of the previous year. The domain used in the calculation of the EOFs is 100 °E to 160 °E, 0°N to 50°N, covering the area where most TCs in this basin are found, and North *et al.*'s, (1982) method is used to estimate the sampling errors in EOFs.

All these predictors are then subjected to a forward stepwise regression analysis, in which they are inserted into a regression equation one by one, retaining each

time the one that contributes the most to increasing the correlation coefficient, R, of the regression equation, until the increase in R^2 of the regression equation by adding a new predictor is less than 0.05. This limit is set to avoid the possibility of overfitting the regression equation (Wilks, 2006). Using this technique, the predictors having the strongest relationship to the behaviour of TCs affecting KJ will be chosen, and the final prediction equation for each scheme will be a weighted linear combination of the respective predictors selected for that scheme. In the following sections, the last number in the abbreviations of the factors indicates the EOF, 1 for the first EOF, 2 for the second, etc., whereas (0) and (−1) after the month indicates the factor is for that month in the current and previous years, respectively.

5.2. Assessing the prediction schemes

The cross-validation technique is used to assess the robustness of the prediction equations derived from a set of dependent samples. The reader is referred to Barnston and van den Dool (1993) for a general description of this technique. Considering the small number of observations in this study, the leave-one-out cross-validation method is used (Michaelsen, 1987), giving 40 new prediction equations for each of the predictions in this study, which in turn gives 40 new predicted number of TCs for each year. These new values are matched against the observed numbers to determine the performance of the prediction equations.

Other ways to evaluate the performance of the schemes include the correlation between the observed values and the hind-casted values, the absolute and root-mean-square errors, and the forecast skill, S. The forecast skill is a measurement of the forecasting performance of a scheme over climatology, and is defined by Wilks (2006) as:

$$S = \left(1 - \frac{RMSE_{Scheme}}{RMSE_{Climatology}}\right) \times 100\%$$

where $RMSE_{Scheme}$ and $RMSE_{Climatology}$ refer to the root-mean-square error of the scheme and climatology, respectively.

Finally, a hind-casted, or predicted number, would be considered acceptable if the value falls within one standard deviation of the observed value during the respective season.

6. Forecasting the number of TCs affecting KJ in different seasons

6.1. Whole season

6.1.1. Predictors

Five predictors are involved in the prediction scheme for N_W, namely, $500U1_{Nov(-1)}$, $500H1_{Feb(0)}$, $500H2_{Sep(-1)}$, $500H2_{Jan(0)}$, and $VOR3_{Feb(0)}$. As suggested by the coefficients of the factors in the prediction equation (Table I), $500H1_{Feb(0)}$ plays the most important role in determining the number of TCs affecting KJ.

Table I. Coefficients of the predictors chosen for the prediction equations for the whole and JN seasons.

Whole season		JN season	
Predictors	Coefficient	Predictors	Coefficient
$500U1_{Nov(-1)}$	−0.822	$500U2_{Feb(0)}$	0.778
$500H1_{Feb(0)}$	−1.695	$850H3_{Feb(0)}$	1.022
$500H2_{Sep(-1)}$	0.791	$850H3_{Apr(0)}$	0.988
$500H2_{Jan(0)}$	0.483	$SHEAR1_{May(0)}$	−0.651
$VOR3_{Feb(0)}$	0.7311	$VOR3_{Mar(0)}$	−1.068
Constant	4.225	Constant	3.800

Figure 7(a) is a scatterplot of the hind-casted and cross-validated numbers as calculated by this scheme *versus* observed number of TCs. The correlation coefficient between the hind-casted and observed numbers of 0.771, which is statistically significant at 95% confidence level, and the forecast skill, S is 36.3% above climatological mean. On the other hand, the correlation coefficient for the cross-validated values and the observed values is 0.673, also significant at the 95% level, while S is 25.2%.

6.2.2. Predicted and cross-validated values for 2004

The year 2004 saw a record breaking number of 10 TCs affecting the KJ region during the whole season. The current prediction scheme is able to capture the above normal N_W, with the predicted value being 7.98, which is within a standard deviation (2.09) of the observed value. The cross-validated value is 7.32. It should be noted that 2004 is a part of the training sample.

6.2.3. Predictions for 2006, 2007, and 2008

Using the current scheme, the predicted N_W is 5.67, 3.79, and 4.17 for the independent samples of 2006, 2007, and 2008 respectively, as opposed to the observed values of 4, 5, and 3. All these 3 predicted values fall within the one standard deviation threshold of 2.00.

6.3. JN season

6.3.1. Predictors

Similar to the N_W prediction scheme, the N_J scheme is comprised of five predictors, namely, $500U2_{Feb(0)}$, $850H3_{Feb(0)}$, $850H3_{Apr(0)}$, $SHEAR1_{May(0)}$, and $VOR3_{Mar(0)}$. The coefficients of the predictors suggest that both $850H3_{Feb(0)}$ and $VOR3_{Mar(0)}$ are important determinants to the number of TCs affecting KJ during this season.

This scheme gives a 95% significant correlation coefficient of 0.817 between the hind-casted and observed numbers, and a forecast skill S of 42.3% above the climatological mean. On the other hand, the correlation coefficient for the cross-validation values and the observed values is 0.749, also significant at the 95% level, and S is 33.3%. Figure 7(b) shows the scatterplot of the

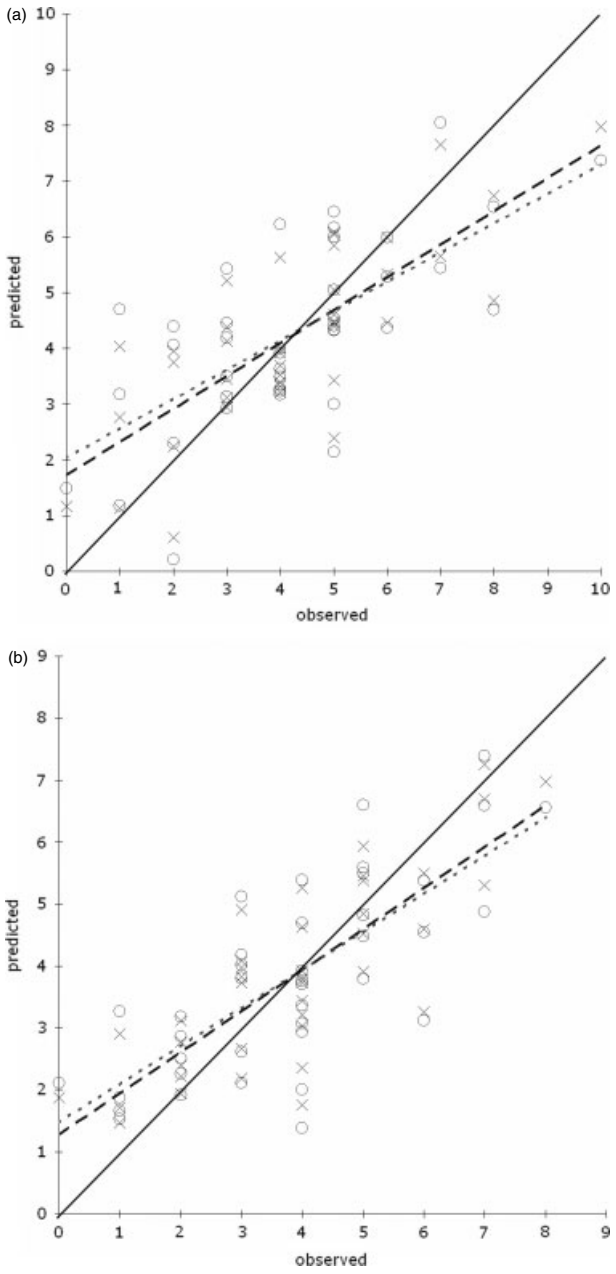

Figure 7. Scatterplots of calculated *versus* observed number of land-falling TCs for the (a) whole and (b) JN seasons. Crosses and dashed line indicate values calculated from the prediction equation and their regression line, while circles and dotted line are cross-validated values and their regression line. The thick diagonal straight line is the 45° line indicating perfect prediction.

hind-casted and cross-validated numbers *versus* observed number of TC for this scheme.

6.3.2. *Predicted and cross-validated values for 2004*

The N_J in 2004 was 8, which is also a record high. The current scheme again is able to capture the higher than normal N_J. The predicted value of 6.97 falls within one standard deviation (1.88) of the observed number. The cross-validated value is 6.56. Again, it should be noted that 2004 is a part of the training set.

6.3.3. *Predictions for 2006, 2007, and 2008*

The predicted N_J is 6.74, 6.00, and 3.40 for the independent samples of 2006, 2007, and 2008, respectively, under this scheme, as opposed to the observed values of 4, 5, and 3. Both the predictions for 2007 and 2008 fall within the one standard deviation threshold of 1.72.

7. Relating the chosen predictors and the TC season

In an attempt to show the relationship between the predictors and the TCs and the related factors, correlation is first drawn between the flow patterns of the predictors and those during the TC season. The values for both the whole and JN seasons are shown in Table II. It can be seen that apart from the vorticity pattern in both seasons, all other factors show statistically significant correlation between the pattern in the month chosen and the one during the respective TC season.

Figures 8 and 9 show the patterns of the factors in years with above- and below-normal number of TCs during the whole and JN seasons, respectively. Focusing first on the whole season, Figure 8 shows that when the number of TCs is above normal, both the patterns of 500H1 (Figure 8(a), left) and 500U1 (Figure 8(c), left) suggest an anomalous easterly flow over the ocean south of Japan, helping to steer TCs in the direction of KJ. At the same time, VOR3 is anomalously positive over the same area (Figure 8(d), left), suggesting favourable conditions for TC genesis. These patterns are reversed when the number of TCs affecting KJ is below normal (Figure 8(a), (c), and (d), right).

On the other hand, in the JN season, when TC number is above normal, the patterns of SHEAR1 (Figure 9(c),

Table II. Correlation between the flow patterns of the predictors chosen for the prediction equations for the whole and JN seasons and the respective patterns during the TC season.

Whole season			JN season		
Predictors	Correlation	Significant?	Predictors	Correlation	Significant?
$500U1_{Nov(-1)}$	−0.392	Yes	$500U2_{Feb(0)}$	0.374	Yes
$500H1_{Feb(0)}$	−0.708	Yes	$850H3_{Feb(0)}$	0.819	Yes
$500H2_{Sep(-1)}$	0.472	Yes	$850H3_{Apr(0)}$	0.770	Yes
$500H2_{Jan(0)}$	−0.391	Yes	$SHEAR1_{May(0)}$	−0.383	Yes
$VOR3_{Feb(0)}$	−0.179	No	$VOR3_{Mar(0)}$	0.147	No

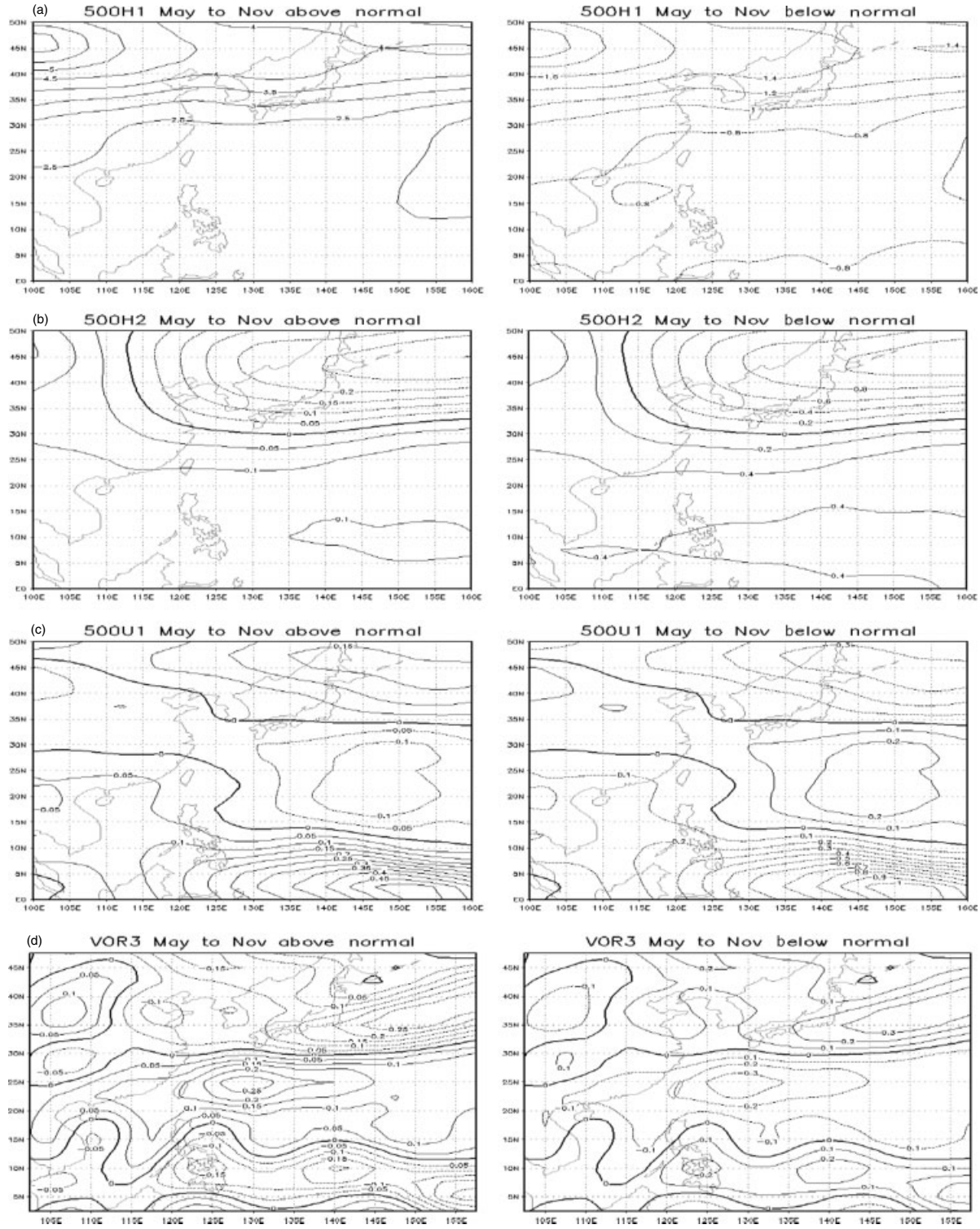

Figure 8. Anomaly patterns of the predictors in the whole season. Solid lines indicate positive values, while dotted lines indicate otherwise. Left panel shows patterns when TC is above normal, whereas right panel is for below normal cases. (a) 500H1 (Unit: gpm), (b) 500H2 (Unit: gpm), (c) 500U1 (Unit: m s^{-1}) (Unit: gpm), and (d) VOR3 (Unit: $\times 10^{-6}$ s^{-1}).

left) and VOR3 (Figure 9(d), left), being negative and positive, respectively, both suggest a favourable environment for TC formation over the ocean south of Japan. Although the pattern of 500U2 (Figure 9(a), left) indicates zonal wind is close to normal in this scenario, it does suggest westerly anomalies when there are below-normal number of TCs affecting KJ (Figure 9(a), right). The patterns of SHEAR1 (Figure 9(c), right) and VOR3 (Figure 9(d), right) are also opposite to the above-normal situation, suggesting unfavourable conditions for TC genesis.

Considering that there are statistically significant correlations between the patterns of the factors in the month

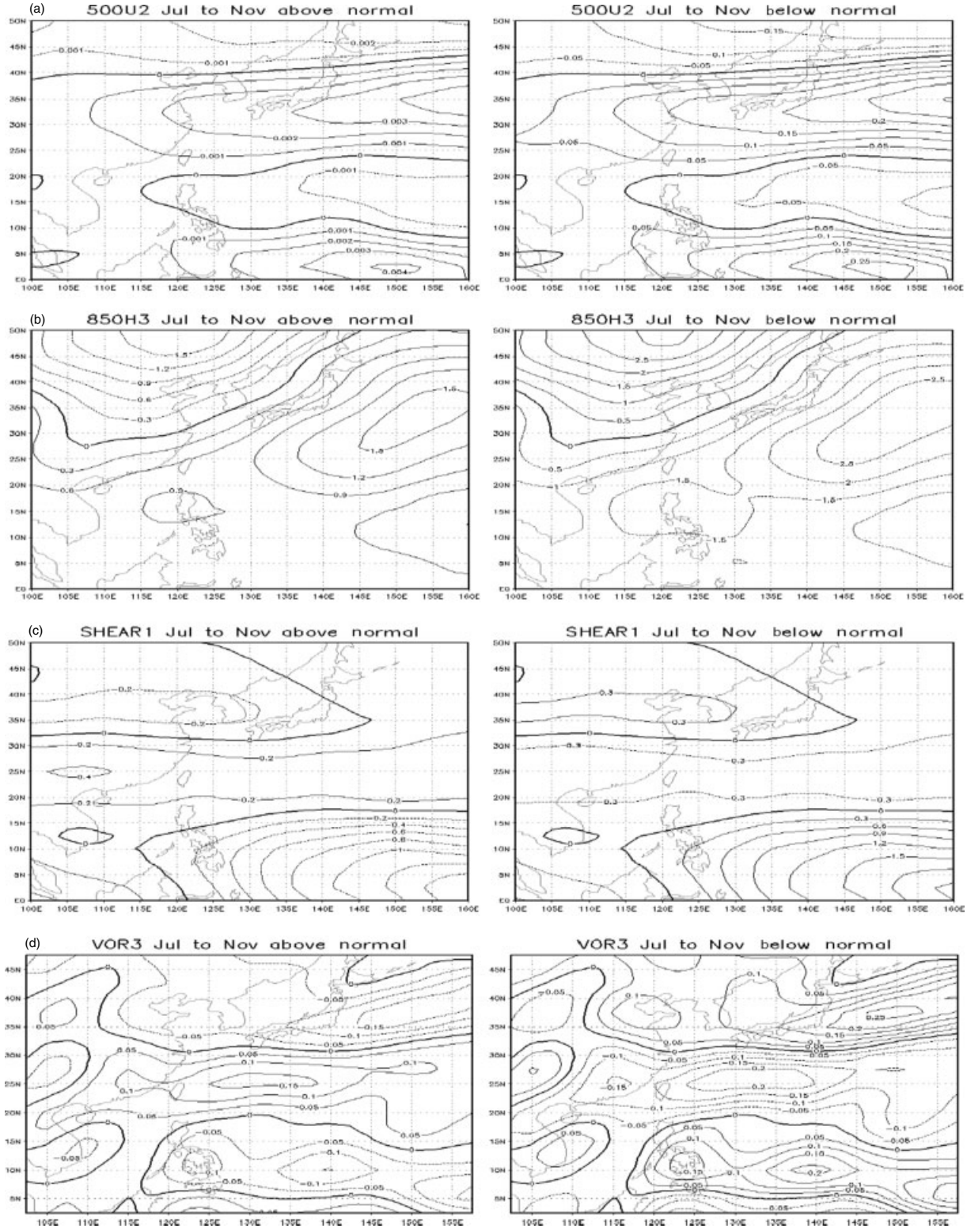

Figure 9. Same as Figure 8 but for the JN season. (a) 500U2 (Unit: m s^{-1}), (b) 850H3 (Unit: gpm), (c) SHEAR1 (Unit: m s^{-1}), and (d) VOR3 (Unit: $\times 10^{-6}$ s^{-1}).

they are chosen as predictors and those during the respective TC seasons, and the ability of the patterns during the TC seasons to explain the observed TC behaviour, it is reasonable to consider that these factors are good to serve as predictors for TC activities in the respective seasons.

8. Summary and discussion

It has long been known that ENSO plays an important role in shaping TC behaviour in the WNP. This study has reconfirmed this assertion, as the number of TCs affecting KJ is shown to be above normal during EN

Table III. Statistics for evaluating the performance of the prediction schemes for the annual number of TCs making landfall over Korea and Japan for the whole and JN seasons.

	Whole season	JN season
Correlation	0.771	0.817
Absolute error	1.60	0.869
Root-mean-square error	1.316	1.073
Forecast skill (%)	36.3	42.3

and lower than normal during LN. The effects of ENSO are seemingly manifested through the modification of the flow patterns, as composite analysis shows the situation during EN to be favourable for TC genesis and tends to cause TCs to re-curve, while the basin provides a relatively less favourable condition for TC formation and a westward steering flow during LN.

Through a forward stepwise analysis, prediction equations are formulated for predicting the number of TCs affecting KJ during the whole and the JN seasons based on the factors found to be related to TC activity in this basin. Results show that the performance of both the schemes is acceptable, reporting forecast skills of 42.3 and 36.3% over climatology, and a 95% significant correlation of 0.817 and 0.771 between the predicted and observed numbers for the whole and JN seasons, respectively (Table III). Moreover, the predicted numbers for 2006, 2007, and 2008 are accurate to within one standard deviation of the observed number, save for that for the JN season in 2006, again indicating a satisfactory performance of the schemes.

That said, a physical reasoning for the choice of these predictors is still absent. Although statistically significant correlations exist between the flow patterns of the predictors during the specific months they are chosen and those when the TCs are actually observed, and the flow patterns during the TC seasons are able to explain the observed TC behaviour, it is difficult to establish causality. It would be worthwhile to investigate further into this topic.

Acknowledgements

The authors would like to thank the Hong Kong Observatory for providing the TC data, the US National Center for Environmental Prediction for the flow pattern data. Fortran program for EOF analysis was developed by David W. Pierce of the Climate Research Division of the Scripps Institution of Oceanography.

References

Barnston AG, van den Dool HM. 1993. A degeneracy in cross-validated skill in regression-based forecasts. *Journal of Climate* **6**: 963–977.

Bove MC, Elsner JB, Landsea CW, Niu X, O'Brien JJ. 1998. Effect of El Niño on U.S. landfalling hurricanes, revisited. *Bulletin of the American Meteorological Society.* **79**: 2477–2482.

Chan CL, Liu KS, Ching SE, Lai ST. 2004. Asymmetric distribution of convection associated with tropical cyclones making landfall along the South China coast. *Monthly Weather Review.* **132**: 2410–2420.

Chan JC-L. 1985. Tropical cyclone activity in the northwest Pacific in relation to the El Niño/Southern Oscillation phenomenon. *Monthly Weather Review.* **113**: 599–606.

Chan JC-L. 2000. Tropical cyclone activity over the Western North Pacific associated with El Niño and La Niña events. *Journal of Climate*. **13**: 2960–2972.

Chan JC-L. 2005. Interannual and interdecadal variations of tropical cyclone activity over the Western North Pacific. *Meteorology and Atmospheric Physics* **89**: 143–152.

Chan JC-L, Xu M. 2009. Inter-annual and inter-decadal variations of landfalling tropical cyclones in East Asia. Part I: time series analysis. *International Journal of Climatology* **29**: 1285–1293.

Choi K-S, Kim D-W, Byun H-R. 2009. Statistical model for seasonal prediction of tropical cyclone frequency around Korea. *Asia-Pacific Journal of Atmospheric Sciences* **45**: 21–32.

Goh AZC, Chan JCL. 2010a. An improved statistical scheme for the prediction of tropical cyclones making landfall in South China. *Weather and Forecasting* **25**: 587–593.

Goh AZC, Chan JCL. 2010b. Interannual and interdecadal variations of tropical cyclone activity in the South China Sea. *International Journal of Climatology* **30**: 827–843.

Gray WM. 1968. Global view of the origin of tropical disturbances and storms. *Monthly Weather Review.* **96**: 669–700.

Gray WM. 1979. Tropical cyclone intensity determination through upper-troposphere aircraft reconnaissance. *Bulletin Of the American Meteorological Society.* **60**: 1069–1074.

Kalnay E, Kanamitsu M, Kistler R, Collins W, Deaven D, Gandin L, Iredell M, Saha S, White G, Woollen J, Zhu Y, Leetmaa A, Reynolds R, Chelliah M, Ebisuzaki W, Higgins W, Janowiak J, Mo KC, Ropelewski C, Wang J, Jenne R, Joseph D. 1996. The NCEP/NCAR 40-year reanalysis project. *Bulletin of the Americla Meteorological Society.* **77**: 437–471.

Kaplan J, DeMaria M. 1995. A simple empirical model for predicting the decay of tropical cyclone winds after landfall. *Journal of Applied Meteorology.* **34**: 2499–2512.

Kim H-S, Ho C-H, Chu P-S, Kim J-H. 2009. Seasonal prediction of summertime tropical cyclone activity over the East China Sea using the least absolute deviation regression and the Poisson regression. *International Journal of Climatology*. DOI:10.1002/joc.1878.

Kimball SK. 2008. Structure and evolution of rainfall in numerically simulated landfalling hurricanes. *Monthly Weather Review.* **136**: 3822–3847.

Lehmiller GS, Kimberlain TB, Elsner JB. 1997. Seasonal prediction models for North Atlantic basin hurricane location. *Monthly Weather Review.* **125**: 1780–1791.

Li C. 1988. Actions of typhoons over the western Pacific (including the South China Sea) and El Niño. *Advances in Atmospheric Sciences* **5**: 107–115.

Liu KS, Chan JC-L. 2003. Climatological characteristics and seasonal forecasting of tropical cyclones making landfall along the South China Coast. *Monthly Weather Review.* **131**: 1650–1662.

Liu KS, Chan JC-L. 2008. Interdecadal variability of Western North Pacific tropical cyclone tracks. *Journal of Climate* **21**: 4464–4476.

Michaelsen J. 1987. Cross-validation in statistical climate forecast models. *Journal of Climate and Applied Meterology* **26**: 1589–1600.

Nakazawa T, Rajendran K. 2007. Relationship between tropospheric circulation over the Western North Pacific and tropical cyclone approach/landfall on Japan. *Journal of the Meteorological Society of Japan* **85**: 101–114.

North GR, Bell TL, Cahalan RF, Moeng FJ. 1982. Sampling errors in the estimation of Empirical Orthogonal Functions. *Monthly Weather Review.* **110**: 699–706.

Santer BD, Wigley TML, Boyle JS, Gaffen DJ, Hnilo JJ, Nychka D, Parker DE, Taylor KE. 2000. Statistical significance of trends and trend differences in layer-average atmospheric temperature time series. *Journal of Geophysical Research.* **105**: 7337–7356.

Shea DJ, Gray WM. 1973. The hurricane's inner core region. I. Symmetric and asymmetric structure. *Journal of the Atmospheric Sciences* **30**: 1544–1564.

Song Y, Lau K-M, Kim K-M. 2002. Variations of the East Asian jet stream and Asian–Pacific–American winter climate anomalies. *Journal of Climate* **15**: 306–325.

Trenberth KE. 1997. The definition of El Niño. *Bulletin of the American Meteorological Society.* **78**: 2771–2777.

Wang B, Chan JC-L. 2002. How strong ENSO events affect tropical storm activity over the Western North Pacific. *Journal of Climate* **15**: 1643–1658.

Wilks DS. 2006. *Statistical Methods in the Atmospheric Sciences,* (2nd edn), Academic Press: St Louis, MO, USA.

Wu MC, Chang WL, Leung WM. 2004. Impacts of El Niño–Southern Oscillation events on tropical cyclone landfalling activity in the Western North Pacific. *Journal of Climate* **17**: 1419–1428.

Wu R, Kinter III JL, Kirtman BP. 2005. Discrepancy of interdecadal changes in the Asian region among the NCEP–NCAR reanalysis, objective analyses, and observations. *Journal of Climate* **18**: 3048–3067.

